Eigenstate structure in graphs and disordered lattices

L. Kaplan*
Institute for Nuclear Theory and Department of Physics, University of Washington, Seattle, Washington 98195
(Received 25 January 2001; revised manuscript received 26 April 2001; published 30 August 2001)

We study wave function structure for quantum graphs in the chaotic and disordered regime, using measures such as the wave function intensity distribution and the inverse participation ratio. The result is much less ergodicity than expected from random matrix theory, even though the spectral statistics are in agreement with random matrix predictions. Instead, analytical calculations based on short-time semiclassical behavior correctly describe the eigenstate structure.

DOI: 10.1103/PhysRevE.64.036225 PACS number(s): 05.45.Mt, 03.65.Sq

Quantum graphs, known also as network models, have been used successfully for many years as simple dynamical systems in which to study complex wave behavior. For appropriate parameter values, graphs can be made to display generic chaotic, disordered, or integrable motion, and at the same time the quantum mechanics of these systems has the simplifying advantage of being semiclassically exact. Originally, graphs were developed as simple models for electronic motion between the atoms of an organic molecule; later it was realized that very similar methods were also applicable to the study of crystalline materials. Seminal work in this field was performed by Pauling as early as 1936 [1], with important later contributions by Coulson [2], by Montroll, who was able to interpolate between free-electron motion and tight-binding models [3], and by Richardson and Balazs, who found a class of networks for which constant energy surfaces were determined entirely by the network topology [4].

The picture developed by these authors is that electrons travel from atom to atom along strictly one-dimensional bonds or pathways (possibly under the influence of a one-dimensional potential), and scatter into other bonds whenever they reach an atomic vertex. Therefore, a key approximation involved in all the graph models is that the potential confining traveling particles to the bonds is strong enough to make excitation of higher-energy transverse modes negligible; similarly the vertices are assumed to behave in a perfectly zero-dimensional manner at relevant energy scales. Apart from this important constraint, one has substantial freedom in choosing the graph topology, the potentials (and possibly also magnetic fields) governing one-dimensional motion along the bonds, and also to some degree the scattering matrix at each vertex, as we will see below.

In the 1980s important progress was made among others by Alexander [5], who used networks to study the behavior of disordered superconductors. Most recently, graph models have been used by a number of authors to study issues as diverse as Anderson localization within the context of periodic orbit theory [6], the spatial distribution and transport properties of persistent currents [7], Aharonov-Bohm conductance modulations in $GaAs/Ga_xAl_{1-x}As$ networks [8], spectral statistics and the trace formula in chaotic systems [9], spectral determinants, with applications to thermodynamic and transport properties of mesoscopic networks [10], and chaotic scattering and resonance behavior [11]. Paralleling this progress of the past several years has been rigorous work on the mathematical structure of graphs, especially that of Carlson, who has studied differential operators on graphs and graph spectral theory [12]. A discussion of the earlier history of quantum graphs can be found in the paper of Kottos and Smilansky [13], which also provides an extensive review of the model.

Though substantial work now exists on the spectral and scattering properties of quantum graphs, and also on their large-scale localization behavior, surprisingly little attention has been paid so far to the detailed wave function structure of this paradigmatic quantum system. In this paper we begin to address questions relating to the statistics of wave functions on graphs and their relation to the underlying classical structures in the system. In the process, we examine the relationship between short-time and long-time effects on stationary behavior, making connections to recent work on other simple quantum chaotic problems, including quantum maps, Sinai billiards, Bunimovich stadia, tunneling in double wells, conductance through chaotic quantum dots, and many-body systems with random two-body interactions [14].

Following the discussion of Ref. [13], a quantum graph consists of V vertices connected by B bonds, each of which is modeled as a one-dimensional wire of length L_j ($j=1,\ldots,B$) along which the wave propagates freely with zero potential. At each of the $i=1,\ldots,V$ vertices, $v_i \geqslant 2$ bonds will meet (note that $\Sigma_{i=1}^{V} v_i = 2B$), and one must impose wave function continuity

$$\Psi_{i,j}(0) = \Psi_{i,j'}(0) \tag{1}$$

and a current conservation condition

$$\sum_j \left(\frac{d}{dx} \Psi_{i,j} \right)(0) = \lambda_i \Psi_{i,j}(0). \tag{2}$$

Note that in both of the equations above we are fixing a vertex i, while j labels the bonds, as it does throughout the paper. $\Psi_{i,j}(x)$ is the wave function in the bond j, with $x=0$ corresponding to the vertex i and $x=L_j$ corresponding to the other vertex. In the continuity condition of Eq. (1), j and j' represent any two bonds meeting at vertex i, while the sum in the current conservation condition of Eq. (2) is over all v_i bonds labeled by j that meet at this vertex. Because of

*Email address: lkaplan@phys.washington.edu

continuity, j on the right-hand side of Eq. (2) can represent *any one* of the bonds meeting at the vertex i; the index j is of course not summed over.

λ_i in the current conservation condition is a free (and possibly energy-dependent) parameter associated with the height of the effective potential at vertex i, and allows one to interpolate between Neumann ($\lambda_i=0$) and Dirichlet ($\lambda_i \to\infty$) boundary conditions. Formally, using self-adjoint extension theory, where one starts out by defining a Hamiltonian operator on the domain of wave functions that live away from the vertices and then classifies all consistent ways of extending this operator to the full domain while keeping it self-adjoint, one can show that the form of Eq. (2) with one free parameter λ is the only one consistent with both wave function continuity and conservation of flux [15,16]. Of course, we also easily see that Eqs. (1) and (2) are invariant under all local permutation of the bonds. In this way, our vertex scatterers are analogous to pointlike s-wave scatterers in empty space, whose strength can similarly be described by a single effective energy-dependent parameter.

Because of time-reversal invariance, the wave function in each bond can be written as $\Psi_{i,j}(x)=a_{i,j}^{(k)}e^{ikx}+a_{i,j}^{(k)*}e^{-ikx}$ for an eigenstate at energy $k^2/2m$. Thus, the distribution of wave function intensities in the system can be completely characterized in the limit $kL\to\infty$ by the distribution of the quantities $|a_{i,j}^{(k)}|^2$. In this limit, the simple normalization condition

$$\sum_{i,j} L_j|a_{i,j}^{(k)}|^2=\sum_j L_j \tag{3}$$

ensures that the mean bond intensity $\langle|a_{i,j}^{(k)}|^2\rangle$ is set to unity.

We begin our analysis with a simple one-dimensional ''ring graph'' [13] where the V vertices are arranged in a circle and each vertex i is connected by bonds to neighboring vertices $i-v/2\ldots i-1,i+1\ldots i+v/2$. v, the number of bonds meeting at every vertex, is known as the valency (here taken to be constant over the entire graph). Setting all the vertex potentials $\lambda_i=0$ leads to the maximum possible delocalization in the graph (the opposite limit, $\lambda_i\to\infty$ would instead produce eigenstates localized on individual bonds), while nonintegrability is ensured through randomness in the bond lengths L_j. In our calculation we take the bond lengths to be uniformly distributed in an interval $[1-\delta L,1+\delta L]$; because the scattering matrices depend only on $kL_j \bmod 2\pi$, all choices of δL are equivalent as long as $\delta L\gg k^{-1}$. The eigenstates of the system may be obtained by examining a $V\times V$ secular matrix $h(k)$ [13]; k is an eigenvalue whenever $\det h(k)=0$, and the associated null vector corresponds to an eigenvector of the graph. In fact, small but nonzero singular values ϵ of $h(k)$ can easily be seen to correspond to eigenvectors of the same system with slightly perturbed potentials $\lambda_i\to\lambda_i-k\epsilon$, so sufficiently small singular values ($|\epsilon|<k^{-1}\lambda$) can also be used to produce eigenstates. This method allows the collection of several independent wave functions at a given value of k for any given realization of the disorder ensemble. One easily checks that collecting one or more wave functions at a given value of k has no discernible effect on the resulting wave function statistics.

Comparing the Heisenberg time ($\hbar$ divided by the mean level spacing, at which individual levels are resolved) with the time required classically to diffuse over the entire system, or alternatively making an analogy with banded random-matrix behavior, we see that the condition for avoiding localization in our system is $v^2\gg V$. We note that the localization condition is k and $\hbar$ independent and depends only on the classical graph geometry. Increasing the valency v for a fixed system size V, one easily observes a transition from localized to delocalized behavior, which can be detected either by looking at the change in level spacing statistics (from Poisson to GOE) or at the change in the wave function intensity correlation (from strongly negative to near zero) between distant points on the graph. Either method confirms the expected scaling behavior for the transition. One can therefore take the large-volume limit $V\to\infty$, where statistical behavior is expected, while easily satisfying the delocalization condition $\sqrt{V}<v\leqslant V-1$.

In this delocalized regime, full information about wave function statistical behavior is contained in the distribution of bond intensities $|a_j^{(k)}|^2$ and their correlations (note that we may freely drop the vertex index i as it is immaterial which of the two endpoints we take to be the beginning of bond j). It is convenient to introduce a simple one-number measure of wave function ergodicity, the inverse participation ratio (IPR),

$$\mathcal{I}=\langle|a_j^{(k)}|^4\rangle, \tag{4}$$

where the averaging is performed over all $B=Vv/2$ bonds j and over a disorder ensemble, at a fixed value of k. Of course, averaging over nearby values of k may also be done. It is often useful to introduce a local version of the IPR, $\mathcal{I}_j$, where the bond j is fixed; then $\mathcal{I}=\langle\mathcal{I}_j\rangle$, averaging over all bonds. The IPR is the first nontrivial moment of the intensity distribution $\mathcal{P}(|a_j^{(k)}|^2)$ (we recall that the mean intensity has been normalized to unity), and can range from 1 in the maximally ergodic case where all intensities are equal up to a maximum value of B in the case of perfect wave function localization on individual bonds. Random matrix theory or the random vector hypothesis would predict Gaussian random fluctuations in the complex coefficients $a_j^{(k)}$, thus $\mathcal{I}=2$. Any enhancement of the IPR above this baseline value indicates a deviation from ergodicity in the local wave function behavior.

The key theoretical idea discussed and applied in several recent works [14] is that wave function intensities in a complex system can often be conveniently separated into a product of short-time and long-time parts,

$$|a_j^{(k)}|^2=\rho_j(E(k))\times r_{jk}. \tag{5}$$

Here $\rho_j(E)$ is a smooth local density of states (known alternatively as the strength function) on the bond j at energy E, obtained as the Fourier transform of the short-time part of the autocorrelation function

$$A_j^{\rm short}(t)=\langle j|e^{-iHt}e^{-t/2T_{\rm cutoff}}|j\rangle, \tag{6}$$

while r_{jk} is obtained (formally) by Fourier transforming the long-time behavior, at times $t\sim T_{\rm cutoff}$ and larger. The decomposition is useful because in many situations the short-time return amplitude $A_j^{\rm short}(t)$ has a known approximate analytical expression, which can be transformed to obtain $\rho_j(E)$. On the other hand, the long-time return amplitude in a chaotic or disordered system is given by a convolution of the short-time behavior with a sum of exponentially many contributions, and thus r_{jk} may be regarded as a random variable

$$\langle r_{jk}\rangle=1,$$

$$\langle r_{jk}r_{j'k'}\rangle=1+(F-1)\,\delta_{jj'}\delta_{kk'}, \tag{7}$$

where the statistical average is performed over an appropriate ensemble. (If r_{jk} is the square of a complex Gaussian random variable, then $F=2$.) Because the smooth local spectral density $\rho_j(E)$ and the fluctuations r_{jk} are associated with distinct time scales (before and after the mixing time, respectively, in a chaotic system), the two quantities are regarded as statistically independent. Thus, for example, the local IPR can be written as

$$\mathcal{I}_j=\langle\rho_j^2\rangle\langle r_{jk}^2\rangle=\langle\rho_j^2\rangle F, \tag{8}$$

where $\langle\rho_j^2\rangle$, the second moment of the smooth local density function, is proportional to the sum of short-time return probabilities $|A_j^{\rm short}(t)|^2$. This formalism has successfully been used to quantitatively study scars of unstable periodic orbits and related phenomena in billiards, in smooth potential wells, and in many-body interacting systems.

To apply these ideas to the ring graphs, we focus on one (arbitrary) bond j connecting vertices 1, 2. An initial wave packet launched in this bond moving from 1 towards 2 will have a probability

$$P_{\rm trans}=v^{-2}\left|1+e^{-2i\tan^{-1}(\lambda_2/vk)}\right|^2 \tag{9}$$

of being transmitted into one of the other $v-1$ bonds meeting at vertex 2; the remaining part of the wave packet then gets reflected back into the original bond [13]. To begin with, we set $\lambda=0$ at all vertices for simplicity, and find that the reflected probability is $P_{\rm refl}=1-(v-1)P_{\rm trans}=1-4(v-1)/v^2$. The process is repeated at vertex 1, and the remaining probability $P_{\rm refl}^2$ travels again the path taken by the original wave packet, leading to a nontrivial contribution to the return probability. We may iterate this process until almost all of the initial probability to be in the bond j has decayed [after $O(1/v)$ bounces for $v\gg1$], and find that the sum of return probabilities behaves as

$$\int dt|A(t)|^2\sim\sum_{t=-\infty}^{\infty}(P_{\rm refl}^2)^{|t|}=\frac{1+P_{\rm refl}^2}{1-P_{\rm refl}^2} \tag{10}$$

(note that we always sum return probabilities over both positive and negative times). To leading order in v, we therefore obtain $\langle\rho_j^2\rangle=v/4-O(1)$ for the short-time factor. Taking into account intermediate-time recurrences (where the wave is transmitted at either vertex into an adjoining bond and is subsequently transmitted back into the bond j) cancels the $O(1)$ term, leading to $\langle\rho_j^2\rangle=v/4+O(v^{-1})$, and thus

$$\mathcal{I}=\mathcal{I}_j=\frac{v}{4}\left(1-\frac{b}{V}\right)F+O(v^{-1}). \tag{11}$$

We note that in Eq. (11) we have included not only $O(v^{-1})$ effects but also the leading finite-volume correction to the semiclassical answer, b being an undetermined dimensionless constant. Since $v^2\gg V$ must hold in order to avoid strong localization, the finite-volume effect is in fact parametrically larger than the finite-v correction, and we therefore omit the latter term in the following. We note also that due to the one-dimensional structure of graphs, Planck's constant can always be scaled out of the problem; therefore the large volume limit plays here the role that the $\hbar\to0$ limit plays in traditional quantum chaotic systems, and finite-volume corrections take the place of leading semiclassical $O(\hbar)$ corrections. These finite-volume corrections are also completely analogous to $O(1/N)$ effects in random matrix theory for $N\times N$ matrices.

The long-time factor F can be obtained directly by measuring the mean square value of $|a_j^{(k)}|^2/\rho_j(E(k))$, i.e., of the bond intensity normalized by the analytically computed short-time spectral envelope. For a wide range of values for the system size V and the valency v, the result $4\leqslant F\leqslant5$ is obtained, supporting the conjecture of independence of short-time and long-time fluctuations in the spectrum (we note $F>2$ means that the long-time fluctuations are super-Gaussian). Numerical data can then be used to fit the coefficient b of the subleading semiclassical correction; the fit is quite good as can be seen in Fig. 1. As expected, the IPR is primarily a function of valency v, with volume dependence being a higher-order effect as long as the delocalization condition $v^2>V$ is satisfied. The wave function statistics clearly deviate strongly from random matrix expectations as v becomes large. This is despite the fact that the level spacing

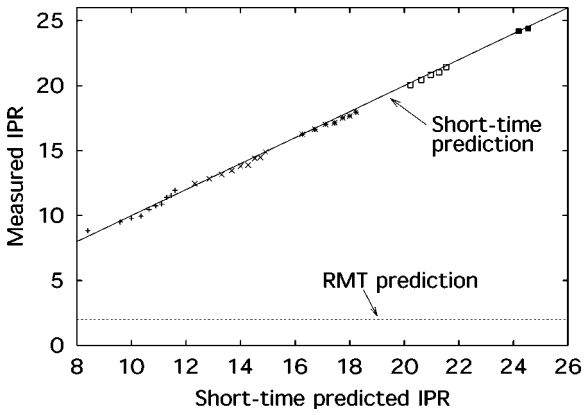

FIG. 1. Observed IPR vs that predicted by the short-time theory, Eq. (11), for ring graphs with parameter values $7\leqslant v\leqslant15$ and $15\leqslant V\leqslant33$. Data points represented by + signs for $v=7$, crosses for $v=9$, stars for $v=11$, empty squares for $v=13$, and full squares for $v=15$.

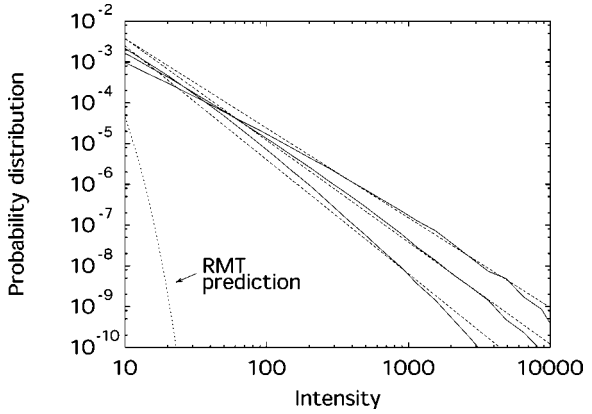

FIG. 2. The tail of the wave function intensity distribution is plotted for a three-dimensional lattice with random potentials λ (see text). From top to bottom, the three solid data curves are for exponent $\alpha=1.2$, 1.5, and 1.8. The corresponding theoretical power laws from Eq. (13) are plotted as dashed lines, with the random matrix theory prediction appearing as a dotted curve for comparison.

statistics of this system are well predicted by random matrix theory, indicating an absence of strong localization.

In a one-dimensional system it is of course impossible to take the semiclassical (large volume) limit for fixed v while staying in the delocalized regime. It is therefore of interest to consider higher-dimensional systems, such as a d-dimensional cubic lattice, with $v=2d$. In the absence of vertex potentials ($\lambda=0$) the above analysis still applies. What happens when we introduce disorder into the system via the potentials λ_i in addition to the disorder already present in the bond lengths? Let the λ_i be independent and distributed for large λ_i in accordance with a power law $\mathcal{P}(\lambda_i)\sim\lambda_i^{-\alpha}$, for $\lambda_0<\lambda_i<\infty$ (with $\alpha>1$). We now claim that the tail of the IPR distribution will be strongly modified by the rare events where a strong potential λ is present on both sides of a given bond j with endpoints 1 and 2. Indeed, we easily see that Eq. (9) for transmission probability reduces to $P_{\rm trans}\sim\lambda^{-2}$ for strong λ. Clearly the weaker of the two potentials λ_1 and λ_2 will dominate the escape rate. The short-time enhancement factor for the local IPR is proportional to the inverse of the escape rate, i.e., $\mathcal{I}_j\sim\min(\lambda_1^2,\lambda_2^2)$, and thus we have the prediction

$$\mathcal{P}(\mathcal{I}_j)\sim\lambda_0^{2(\alpha-1)}\mathcal{I}_j^{-\alpha} \tag{12}$$

for $1\ll\mathcal{I}_j\ll V$, modifying the exponential fall off predicted by random matrix theory. Similarly, the tail of the intensity distribution becomes

$$\mathcal{P}(|a|^2)\sim\lambda_0^{2(\alpha-1)}(|a|^2)^{-\alpha-1} \tag{13}$$

for $1\ll|a|^2\ll V$, in contrast with the exponential Porter-Thomas prediction valid for a system satisfying random matrix statistics.

The result of Eq. (13) is confirmed in Fig. 2, where we have used an ensemble of 37^3 lattices with one out of every $D=11$ sites randomly chosen to contain a scatterer (the particle executes free motion while traveling between the scatterer sites, so that the classical motion is diffusive with diffusion constant growing with D). The total number of scatterers is then $V=4604$, and we indeed see that the data curves tend quickly to zero for $|a|^2\geqslant V$. We have checked that with increasing number of scatterers V at fixed α, the intensity distribution curves keep following a given power law behavior for larger and larger intensity, before eventually dropping off to zero. Similarly, we have checked that varying D by a factor of 2 does not significantly affect the intensity distribution for fixed V, as would have been expected for a diffusion-dominated logarithmic-normal tail, $\log\mathcal{P}\sim-D\log^2(|a|^2)/\log V$ [17,18]. We see instead that the tail of the intensity distribution is dominated entirely by the short-time system behavior.

TABLE I. Numerically obtained inverse participation ratio $\mathcal{I}$ for a disordered three-dimensional lattice with exponent $\alpha=1.5$, compared with the prediction of Eq. (14) for various numbers of scatterers V, mean scatterer spacings D, and minimum potential values λ_0. The constant used is $C_\alpha=3.0$.

V	D	λ_0	$\mathcal{I}_{\rm predicted}$	$\mathcal{I}_{\rm actual}$
549	4	0.3	21	23
549	4	1.0	70	72
2197	8	1.0	141	137
2315	4	1.0	144	131
4604	11	1.0	204	210

Finally, we return to the volume-averaged IPR $\mathcal{I}$, the simplest overall measure of the degree of wave function localization. From Eq. (12), we easily obtain in the large-volume limit

$$\mathcal{I}=C_\alpha\lambda_0^{2(\alpha-1)}V^{2-\alpha} \tag{14}$$

for $1<\alpha<2$. As we can see in Table I, this result compares favorably to the numerically computed value over a range of volumes V and for different mean scatterer spacings D and minimum potentials λ_0. None of the IPR's are close to the random matrix prediction $\mathcal{I}=2$.

In conclusion, we have seen that various aspects of wave function structure in chaotic and disordered quantum graphs are adequately described using the analytically known short-time behavior of the system, specifically the return amplitude at short times and its Fourier transform. On the other hand, random matrix theory completely fails to describe the wave function structure, even though its predictions are good for the spectral statistics. This failure can be understood as resulting from the omnipresence of short periodic orbits in graphs, in contrast with the situation prevailing in most other chaotic systems.

Several very valuable discussions with T. Kottos are gratefully acknowledged. This work was supported by the DOE under Grant No. DE-FG03-00-ER41132.

[1] L. Pauling, J. Chem. Phys. **4**, 673 (1936).
[2] C. A. Coulson, Proc. Phys. Soc. London **67**, 608 (1954).
[3] E. W. Montroll, J. Math. Phys. **11**, 635 (1970).
[4] M. J. Richardson and N. L. Balazs, Ann. Phys. (N.Y.) **73**, 308 (1972).
[5] S. Alexander, Phys. Rev. B **27**, 1541 (1985).
[6] H. Schanz and U. Smilansky, Phys. Rev. Lett. **84**, 1427 (2000).
[7] M. Pascaud and G. Montambaux, Phys. Rev. Lett. **82**, 4512 (1999).
[8] J. Vidal, G. Montambaux, and B. Doucot, Phys. Rev. B **62**, R16 294 (2000).
[9] H. Schanz and U. Smilansky, Philos. Mag. B **80**, 1999 (2000).
[10] E. Akkermans, A. Comtet, J. Desbois, G. Montambaux, and C. Texier, J. Phys. A **33**, L63 (2000).
[11] T. Kottos and U. Smilansky, Phys. Rev. Lett. **85**, 968 (2000).
[12] R. Carlson, Electron. J. Differential Equations **23**, 1 (1997); **6**, 1 (1998).
[13] T. Kottos and U. Smilansky, Ann. Phys. (N.Y.) **274**, 76 (1999).
[14] L. Kaplan and T. Papenbrock, Phys. Rev. Lett. **84**, 4553 (2000); L. Kaplan and E. J. Heller, Phys. Rev. E **62**, 409 (2000); L. Kaplan, *ibid.* **62**, 3476 (2000); W. E. Bies, L. Kaplan, M. R. Haggerty, and E. J. Heller, *ibid.* **63**, 066214 (2001); W. E. Bies, L. Kaplan, and E. J. Heller, *ibid.* **64**, 016204 (2001); L. Kaplan, Phys. Rev. Lett. **80**, 2582 (1998).
[15] P. Exner and P. Seba, Rep. Math. Phys. **28**, 7 (1989).
[16] J. Gratus, C. J. Lambert, S. J. Robinson, and R. W. Tucker, J. Phys. A **27**, 6881 (1994).
[17] V. I Fal'ko and K. B. Efetov, Phys. Rev. B **52**, 17 413 (1995).
[18] I. E. Smolyarenko and B. L. Altshuler, Phys. Rev. B **55**, 10 451 (1997).